Scanning Electrochemical Microscopy. 22. Examination of Thin Solid Films of AgBr: Ion Diffusion in the Film and Heterogeneous Kinetics at the Film/Solution Interface

Michael V. Mirkin, Meral Arca,† and Allen J. Bard*

Department of Chemistry and Biochemistry, The University of Texas at Austin, Austin, Texas 78712

Received: June 2, 1993; In Final Form: July 27, 1993®

A new approach to the characterization of thin solid films, based on the use of the scanning electrochemical microscope (SECM), is described. Parameters of interest, e.g., the heterogenous rate constant for a chemical reaction at the film/solution interface and the diffusion coefficient of species inside the film, can be determined from the SECM approach curves. The analysis of the SECM current–distance curves also provides information about the spatial localization of a chemical (or electrochemical) reaction (i.e., at the substrate/film vs the film/solution interface). Silver bromide films electrodeposited on a silver substrate were used as a model experimental system to test this method, with determination of the diffusion coefficient of bromide ion in the AgBr layer (5.6×10^{-7} cm^2/s) and the heterogenous rate constant for the reaction of AgBr with hexaammineruthenium(II) (0.082 cm/s). The latter reaction occurs at a film/solution interface, in contrast with the electroreduction of tris(2,2′-bipyridyl)osmium(II) which occurs at the silver substrate surface via diffusion through pores in the AgBr film rather than at the highly resistive AgBr/solution interface.

Introduction

Various approaches to studies of the dynamic behavior of thin electroactive films[1] and the related capabilities of the scanning electrochemical microscope (SECM)[2] have been reviewed recently. The responses of two working electrodes, the SECM tip ultramicroelectrode and the substrate electrode modified with the film of interest, can provide a more comprehensive view of the often complicated metal/film/solution system than electrochemical studies of the modified electrode alone. In addition to the modified substrate electrode response that mainly reflects processes at the metal/film interface, the SECM tip can probe the film/solution interface directly from the solution side. This allows better qualitative and quantitative descriptions of such phenomena as adsorption/desorption kinetics,[3] counterion ejection and incorporation,[4] and heterogeneous processes at enzyme-modified electrodes.[5]

This paper deals with three problems related to the characterization of thin films. The first pertains to the spatial localization of chemical or electrochemical reactions. Although in some cases the locale of a reaction is clear (e.g., when anions cannot penetrate a Nafion film due to Donnan exclusion, the electrooxidation of $IrCl_6^{3-}$ occurs only at the film/solution interface[6]), for other systems the site of the reaction is not obvious. In that case, the high spatial resolution offered by the SECM can be helpful. An SECM approach (current–distance) curve[7] represents the steady-state tip current (i_T) as a function of the tip–substrate distance (d). In SECM theory, d is the distance between the tip and the plane where the regeneration of the mediator occurs (for an electronically conductive substrate) or the blocking plane (for an insulating substrate). The concept is clear with a flat unmodified substrate (e.g., a metal) but not for a substrate modified with a thin film. In the latter case, several different situations can be considered. (i) The regeneration of the mediator occurs at a film/solution interface (Figure 1A). The position of the substrate obtained from the SECM approach curve (the zero-distance point) coincides with the z coordinate of the film/solution interface (this usually can be found as the point where the tip touches the substrate) as long as the mediator regeneration is fast. Here, the shape of i_T–d curves is independent of the film thickness. (ii)

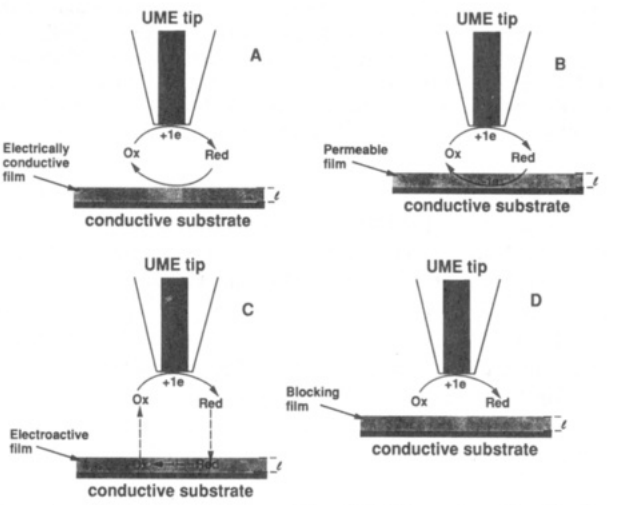

Figure 1. Schematic diagrams of the SECM experiments with four different types of mediator regeneration. (A) Regeneration of a mediator at a film/solution interface via heterogeneous chemical or electrochemical reaction (case i in the text). (B) Electrochemical regeneration of a mediator at a conductive substrate surface (case ii in the text). (C) Regeneration proceeds by reaction between film and tip generated species at the surface or within the film (case iii in the text). (D) Regeneration of a mediator at a substrate is blocked by resistive and impermeable film, resulting in negative feedback due to the hindered diffusion of redox species to the tip electrode (case iv in the text).

The mediator is regenerated at the metal/film interface (Figure 1B). If the tip does not penetrate the film, the maximum feedback current magnitude decreases with an increase in the film thickness, l, and no positive feedback current is obtained when $l \gg a$ (where a is the tip radius). The substrate position obtained from the i_T–d curve with positive feedback relates to the metal/film, rather than the film/solution, interface. If the diffusion coefficients of the mediator in solution and in the film are similar, the film thickness can be evaluated as a difference of the coordinates of the metal/film and film/solution interfaces. (iii) The regeneration proceeds by reaction between film and tip generated species at the film/solution interface or within the film (Figure 1C). In this case, the zero-point on the i_T–d curve does not correspond to either the inner or outer boundary of the film and the approach curve shape deviates significantly from simple SECM theory. Unlike case ii, the positive feedback current does not vanish with

† Permanent address: Hacettepe University, Chemistry Department, 06532 Beytepe, Ankara, Turkey.

® Abstract published in *Advance ACS Abstracts,* September 15, 1993.

0022-3654/93/2097-10790$04.00/0

an increase in l as long as charge transport in the film is rapid. (iv) When no regeneration occurs at the film/solution interface (Figure 1D) and the coating is impenetrable to the mediator (or so compact that mediator diffusion inside the film is slow), the substrate appears as an insulating one and the zero-point on the i_T–d curve corresponds to the outer film boundary. Thus, by using the shape of the SECM approach curves one can investigate spatial localization and, sometimes, the mechanism of the redox reaction at a thin film modified surface. In this study, we illustrate this methodology with a Ag substrate covered with a several-micron-thick AgBr film and demonstrate with the help of the SECM that the chemical reaction of AgBr with $Ru(NH_3)_6^{2+}$ occurs at the film/solution interface (case i), that the electroreduction of $Os(bpy)_3^{3+}$ can take place only at the silver substrate surface, and that the highly resistive AgBr layer blocks this process (case iv).

A second problem of interest is the evaluation of rate constants of fast heterogeneous chemical reactions. Unlike heterogeneous electrochemical kinetic parameters which can be extracted from dc or ac current–potential curves, chemical reactions at interfaces are not directly accessible, and the study of the kinetics as a rate-determining stage of a complex process is not straightforward.[6,8] Previously,[9,10] we demonstrated the suitability of the SECM for the determination of the rate constants for quasi-reversible and irreversible electron-transfer reactions at tip and substrate electrodes. Here, we demonstrate a simple and reliable methodology for extraction of the rate constant (k) of a heterogeneous chemical reaction from steady-state SECM current–distance curves similar to the approach used previously in studies of fast electron transfer.

The last question addressed here, the evaluation of the diffusion coefficient (D) of a species inside a film cast on an electrode, has been treated extensively in the literature.[1] If the species of interest participates in an electrode reaction, the value of D can be deduced from the diffusion plateau current (e.g., at an RDE[11]), which is proportional to D under suitable conditions, from chronocoulometric data,[12] or from ac measurements.[13] The analysis of such data may not be straightforward, because the overall process comprises a number of stages, including diffusion in solution, charge transfer or extraction at the film/solution interface, mass-transfer and electron-transfer reactions within the film, movement of co-ions, and heterogeneous electron transfer at the film/solution interface. Murray et al.[14,15] introduced several "solid-state" approaches, such as microelectrode voltammetry in a redox film, interdigitated electrode arrays, and various twin-electrode thin-layer devices where an electroactive film is sandwiched between two electrodes to determine diffusion coefficients. In these experiments, problems caused by solution processes are largely eliminated. In a similar way, the determination of the apparent diffusion coefficient for a redox species in a polyelectrolyte was carried out with a small (30-nm base radius) conical electrode penetrating the film.[16] Most of these techniques, however, cannot be used to determine diffusion coefficients of species that are not electroactive in the film (although a sandwich-type device, an ion-gate electrode,[15b] was employed to evaluate chloride conductivities of oxidized and reduced polypyrrole). There are also many systems of interest which cannot be studied by any of the above methods. For example, hard films such as salts or oxides are not suitable for penetration experiments, and the construction of sandwich electrodes with these is difficult. Here, we propose an approach based on the evaluation of the time required for a species to cross the tip/substrate gap. Conceptually, this method is similar to a time-of-flight experiment[14c] but offers somewhat better defined geometry and does not require the preparation of a sandwich electrode configuration.

Experimental Section

Chemicals. $Ru(NH_3)_6Cl_3$ (Strem Chemicals, Newburyport, MA), KNO_3 (EM Science, Gibbstown, NJ), and HBr (Fisher Scientific, Fair Lawn, NJ) were used as received. Tris(2,2′-bipyridyl)osmium(II) ($Os(bpy)_3^{2+}$) was synthesized according to previously reported procedures.[17] Aqueous solutions were 5 mM in $Ru(NH_3)_6^{3+}$ or 2 mM in $Os(bpy)_3^{2+}$ and 0.5 M in KNO_3. All solutions were prepared with deionized water (Milli-Q, Millipore Corp.).

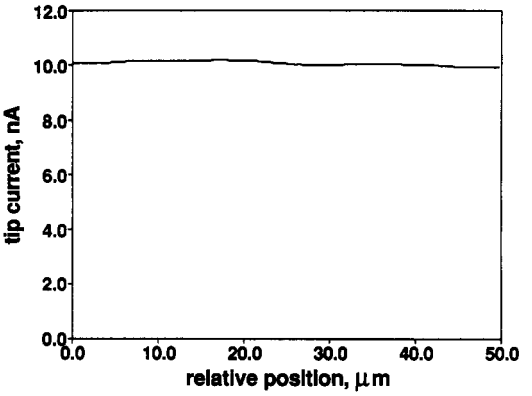

Figure 2. Steady-state tip current as a function of relative tip position over a 5-μm-thick AgBr layer. A 10-μm-diameter Pt tip was scanned laterally at 5 μm/s. Solution contained 5 mM $Ru(NH_3)_6^{3+}$ and 0.5 M KNO_3. The tip was about 5 μm away from the silver bromide layer. Tip potential, E_T = –450 mV vs SCE; unbiased substrate.

Electrodes. A 10-μm-diameter Pt microdisk tip was fabricated as described previously[18] and was polished with 0.05-μm alumina before a set of measurements. Data were acquired with either a three- or a four-electrode configuration (with a Pt wire serving as a counterelectrode, an SCE reference electrode, and with the substrate electrode either biased or unbiased). A 1-mm-diameter Ag wire (Aldrich Chemical Co., Milwaukee, WI) was sealed in glass, polished with 0.05-μm alumina, and used as a substrate for the electrodeposition of AgBr.

The SECM apparatus was described previously.[19] The SECM measurements were performed in a 3-mL Teflon cell. A PAR (Princeton Applied Research, Princeton, NJ) Model 175 programmer was used to generate potential pulses in time-of-flight measurements. The approach curves and transients were obtained using an EI-400 four-electrode potentiostat (Ensman Instruments, Bloomington, IN).

Preparation and Preliminary Characterization of AgBr Films. Electrodeposition of AgBr on a 1-mm-diameter silver substrate was carried out in 1 M HBr solution with a BAS-100A electrochemical analyzer (Bioanalytical Systems, West Lafayette, IN) used in the bulk electrolysis mode at 0.5 V vs SCE. The thickness of the AgBr layer (l) was calculated as a function of the electric charge passed (Q), electrode surface area (A = 0.007 85 cm^2), the density of silver bromide (ρ = 6.473 g/cm^3),[20] and its molecular weight (m = 187 g/mol) by the expression

$$l = Qm/(F\rho A) = 0.0382Q \quad (1)$$

The amounts of charge required to obtain 2-, 10-, 20-, and 40-μm-thick AgBr films were thus 5.2, 26, 52, and 104 mC, respectively. The AgBr films formed in this way were smooth on the micrometer scale, as shown by the SECM curve obtained by scanning the tip laterally over a 50-μm length of the film (Figure 2). The essentially constant tip current obtained is consistent with a film roughness in the submicrometer range.

The agreement between the actual thicknesses of the AgBr films and those calculated by eq 1 was checked as follows. One-half of the circular Ag substrate was painted with high-voltage insulating lacquer (Micro Super XP Stop-Off, Tolber, Hope, AR). The other half was covered with AgBr by passing an amount of charge corresponding to the desired thickness. The resin was then peeled off and the composite substrate was examined with the SECM with $Ru(NH_3)_6^{3+}$ as mediator. The thickness of the AgBr film was obtained as a difference between z coordinates of

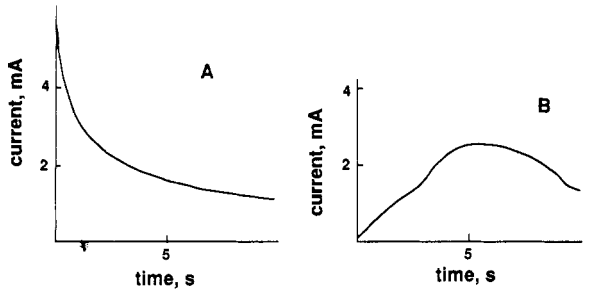

Figure 3. Chronoamperograms for (A) oxidation of silver in 1 M HBr and (B) reduction of silver bromide. The potential of the 1-mm-diameter Ag disk electrode was stepped to +500 mV vs SCE (A) and then to −400 mV (B).

the insulating film surface and the bare silver. For two values of the passed charge (12.1 and 26.4 mC) the calculated and SECM values of l were 8.3 vs. 7.7 μm and 20.0 vs 19.1 μm, respectively. This difference is within expected experimental error, so given film values imply an uncertainty of about 5–10%.

The films of AgBr were found by the SECM experiments to be very electrically resistive, in agreement with literature data (conductivity, $\kappa = 1.7 \times 10^{-7}\ \Omega^{-1}\ cm^{-1}$).[21] The shapes of formation and dissolution transients (Figure 3) are in good qualitative agreement with those calculated for thin-layer systems with a varying ohmic resistance,[22] although a quantitative comparison was not carried out because of the complexity of the film nucleation/growth mechanism. During the AgBr formation step, the resistance increased with time, and the current decreased monotonically (Figure 3A). During the reduction of the AgBr film, the thickness of the layer decreased, causing a decrease in the resistance. This process typically resulted in chronoamperometric curves showing a peak (Figure 3B).

Results and Discussion

Spatial Localization and Mechanism of the Heterogeneous Chemical AgBr Reduction Reaction. Two SECM current–distance curves obtained with a Ag/AgBr substrate and different redox mediators, (A) $Os(bpy)_3^{2+}$ and (B) $Ru(NH_3)_6^{3+}$, are shown in Figure 4. Figure 4A clearly displays negative feedback, and the data can be fit quantitatively to the theory of the SECM with an insulating substrate.[7] This redox mediator in SECM experiments with conductive (metal) substrates produces a positive feedback current[16] with the substrate reaction:

$$Os(bpy)_3^{3+} + e = Os(bpy)_3^{2+} \qquad E^{\circ\prime} = 0.84\ V\ vs\ NHE \tag{2}$$

Clearly, the compactness of the silver bromide layer diminishes mediator diffusion to the Ag substrate, and its low electronic conductivity makes the rate of the process (eq 2) at the AgBr/solution interface negligibly small. Moreover, because the $E^{\circ\prime}$ for the Ag/AgBr half-reaction is 0.071 V vs NHE, AgBr does not react with either the Os(II) or Os(III) forms. As a result, even a 2-μm-thick film ($l < a$) appears blocking.

The approach curve in Figure 4B is very different. A positive feedback current is shown; this increases as the tip approaches the film, attaining a value of $I_T \cong 4$ (where the normalized feedback current $I_T = i_T/i_{T,\infty}$; i_T is the tip current at distance d and $i_{T,\infty}$ is the steady-state diffusion current with the tip electrode far from the substrate). At smaller d, contact between the tip and AgBr causes a very sharp increase in the tip current as the tip electrode causes direct reduction of AgBr. This allows precise determination of the d = 0 point. The value of $I_T = 4$ corresponds to a tip–substrate separation of the order of 1 μm (for $a = 5$ μm) and, because $l = 10$ μm, completely eliminates the possibility of mediator regeneration occurring at the metal/film boundary. The above findings, as well as the essential independence of the shape of approach curves on l (compare parts A and B of Figure 5), show that $Ru(NH_3)_6^{3+}$ is regenerated at the film/solution interface. Since silver bromide is highly resistive, the regeneration is not an electrochemical process like reaction 2, with electron transfer through the AgBr film, but rather a heterogeneous chemical reaction. The positive SECM feedback is due to the following processes:

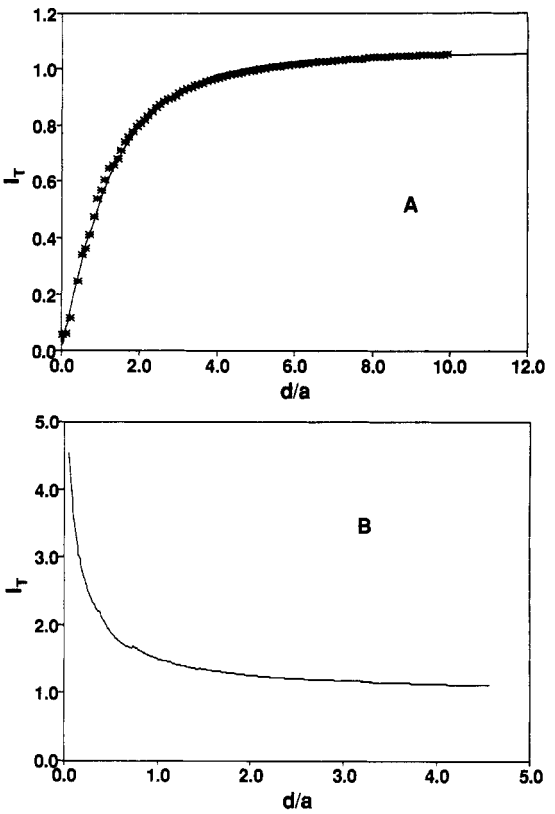

Figure 4. SECM approach curves obtained with a 10-μm-diameter Pt tip over a Ag/AgBr substrate. Solution contained (A) 2 mM $Os(bpy)_3^{2+}$ in 0.5 M KNO_3 and (B) 5 mM $Ru(NH_3)_6^{3+}$ in 0.5 M KNO_3. The thickness of the AgBr layer was 2 μm (A) and 10 μm (B). Solid line in (A) represents the theory for a diffusion-controlled process in SECM with an insulating substrate.[7] The zero-point corresponds to the AgBr/solution boundary. The tip potential was +0.8 V vs SCE (A) and −0.45 V (B) where the tip processes were diffusion-controlled and the tip approached the substrate at a rate of 0.1 μm/s. Small discontinuities are artifacts caused by piezo clicks.

$$Ru(NH_3)_6^{3+} + e = Ru(NH_3)_6^{2+} \qquad E^{\circ\prime} = 0.05\ V\ vs\ NHE\ (tip\ process) \tag{3a}$$

$$AgBr + Ru(NH_3)_6^{2+} \xrightarrow{k} Ag + Br^- + Ru(NH_3)_6^{3+} \qquad (substrate\ process) \tag{3b}$$

Schematic diagrams of the SECM experiments with the redox mediators thus correspond to those shown in Figure 1C ($Ru(NH_3)_6^{3+}$) and Figure 1D ($Os(bpy)_3^{3+}$).

SECM Determination of the Rate Constant of an Irreversible Heterogeneous Chemical Reaction. We now develop an approach to the determination of heterogeneous chemical rate constants from SECM data. Because of the formal similarity between the electrochemical and chemical regeneration of the redox mediator (Figure 1A,C), the procedure is similar to that proposed earlier[9,23] for heterogeneous electrochemical processes. There are, however, some differences. The electrochemical procedure was developed to analyze kinetics of the tip process, while here it is the substrate reaction that is of interest. Moreover, for an electrochemical process, the rate constant is a function of the electrode potential, while for a chemical process, k is potential-independent.

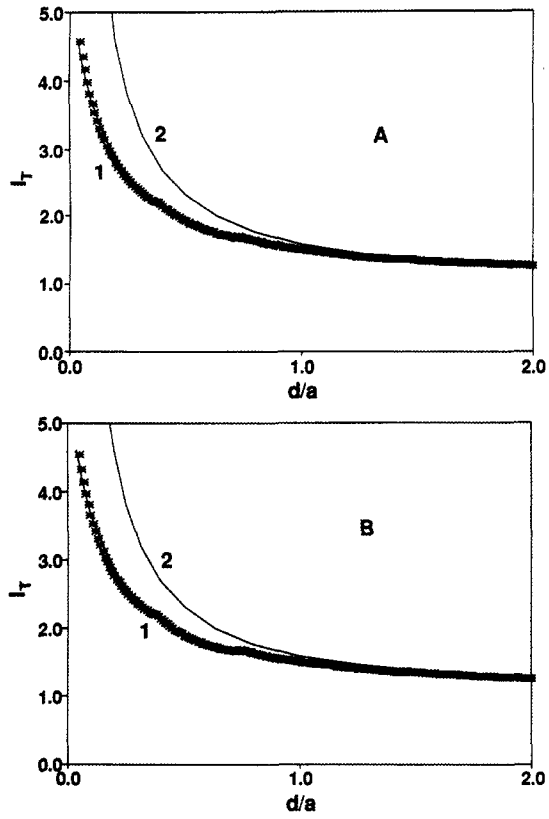

Figure 5. SECM approach curves with positive feedback caused by chemical regeneration of $Ru(NH_3)_6^{3+}$ at a AgBr-covered substrate. Theoretical curves (solid line) were computed from eq 11 with $k/D = 1.25 \times 10^4$ for the substrate chemical reaction (curves 1), compared to that for a diffusion-controlled substrate process (curves 2). The thicknesss of the AgBr layer was (A) 10 μm and (B) 40 μm. Other parameters as in Figure 4.

First let us derive an analytical approximation for a current–distance SECM curve (I_T–d) with finite irreversible substrate kinetics. As in ref 9, we make use of the expression for a diffusion-controlled tip current:

$$i_T = i_{TLC}(L) + i'(L) \tag{4}$$

where $L = d/a$ is the normalized tip–substrate separation. The first term on the right-hand side of eq 4 represents the diffusion-limiting current in a thin-layer cell (TLC) with a working electrode surface area $A = \pi a^2$:[24]

$$i_{TLC} = \pi nFc^\circ Da/L \tag{5}$$

The second term in eq 4 accounts for the difference between the SECM current and that of a thin-layer cell with the same gap width because of diffusion of material into the gap:[23,25]

$$i' = i_{T,\infty}[0.68 + 0.3315 \exp(-1.0672/L)] \tag{6}$$

where $i_{T,\infty}$ is[26]

$$i_{T,\infty} = 4nFDc^\circ a \tag{7}$$

and c° is the bulk concentration of the redox mediator. The term i' represents the contribution of the microdisk steady-state current to the total current diminished by the blocking effect of the substrate plus a small part of the feedback current associated with the substrate surface beyond the circle of radius a facing the tip. The smaller is L, the smaller is the relative contribution of i' to the SECM current. Assuming the diffusion coefficients of oxidized and reduced species are equal, so that $c_{Ox} + c_{Red} = c^\circ$ everywhere in the cell, one can write the following expression for the TLC current when it is limited by the rate of the first-order irreversible heterogeneous reaction:

$$i^k_{TLC} = nFAkc_{Red} = nFAD(c^\circ - c_{Red})/d \tag{8}$$

where c_{Red} is the concentration of the reduced species at the substrate surface. After simple transformations, one can express the TLC current as a function of the kinetic parameter $\Lambda_c = kd/D$:

$$i^k_{TLC} = i_{TLC}/(1 + 1/\Lambda_c) \tag{9}$$

Since i' can be taken as independent of the substrate reaction rate, eq 9 can be combined with eq 4 to yield the following expression for the tip current:

$$i^k_T = \frac{i_T}{(1 + 1/\Lambda_c)} + \frac{i'}{(1 + \Lambda_c)} \tag{10}$$

or, after normalization by $i_{T,\infty}$,

$$I^k_T = \frac{I_T}{(1 + 1/\Lambda_c)} + \frac{I'}{(1 + \Lambda_c)} \tag{11}$$

where I^k_T is the normalized tip current under kinetic control, $I' = i'/i_{T,\infty}$, and the normalized diffusion-controlled tip current is $I_T = i_T/i_{T,\infty}$. This approximation is sufficiently accurate when the chemical reaction is fast.

The two experimental approach curves presented in Figure 5 were obtained with a Pt tip over the substrate covered with AgBr in a solution containing 5 mM $Ru(NH_3)_6^{3+}$. As shown above, the feedback current in this system is due to the heterogeneous chemical reaction in eq 3b. The rate constant for this reaction can be obtained by fitting the experimental current–distance curves to the theoretical one with a simple adjustable parameter, Λ_c. As expected, the same value of $k = 0.082$ cm/s (with $D = 6.3 \times 10^{-6}$ cm^2/s for $Ru(NH_3)_6^{3+}$)[9] was extracted from both approach curves obtained with substantially different thicknesses of AgBr film, i.e., $l = 10$ μm (Figure 5A) and $l = 40$ μm (Figure 5B).

Time-of-Flight Experiments with the SECM. Various approaches to the determination of the diffusion coefficient (either the actual D for physical diffusion or an effective diffusion coefficient for an electron hopping process) from the time required for an electroactive species to cross the gap between generator and collector electrodes have been proposed previously.[14c,27,28] All of these are based on the equation

$$t_x = \text{const } d^2/D \tag{12}$$

which can be considered as a corollary of the Einstein equation.[29] t_x is the characteristic time, d is the generation–collector distance, and const is an empirical constant. Although different time-related parameters were used as t_x (i.e., the time corresponding to the maximum of the collector transient,[14c,27a] the time corresponding to $^1/_3$ or $^2/_3$ of the quasi-steady-state collection current,[27] or the "critical time" that is relevant to the point where an SECM transient deviates from that of a microdisk electrode[28]) with different values for the proportionality constant, const, all of these are related to the particular geometry of the situation.

Our procedure is conceptually similar to the time-of-flight experiment in ref 14c. The tip was positioned in close proximity to the substrate and the tip–substrate separation was determined from the zero-point using the piezo calibration. Tip and substrate transients, following the application of a short potential pulse to the substrate electrode to produce a diffusion-controlled reaction, were recorded, and the time corresponding to the maximum tip current, t_{max}, was determined from the digitized data.

Feldman et al.[14c] found by digital simulation for a twin-electrode TLC a const = 0.17. A similar value is expected with SECM at very close tip–substrate separations ($d \ll a$) when the SECM behavior is essentially that of a TLC (i.e., i' in eq 4 is negligible).

TABLE I: Calibration for SECM Time-of-Flight Experiments[a]

Δt, ms	ν, Hz	t_{max}, s
5	no	1.5 ± 0.3
5	7	1.4 ± 0.2
10	15	1.3 ± 0.15
20	20	1.4 ± 0.1
50	20	1.3 ± 0.05

[a] Peak times t_{max}, in time-of-flight experiments with a Pt substrate and $Ru(NH_3)_6^{3+/2+}$ mediator, obtained at d = 85.7 μm with different values of pulse width Δt and potentiostat filter frequency ν. For other conditions, see Figure 6.

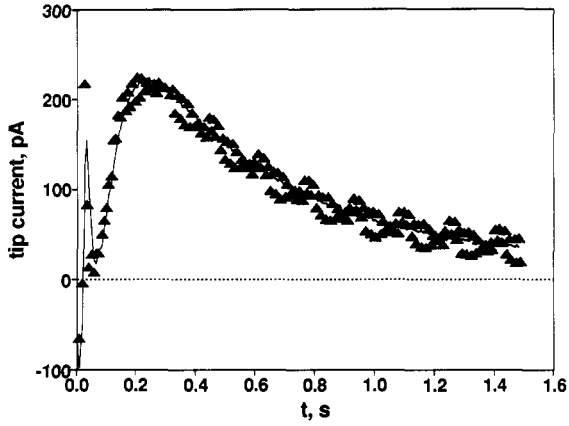

Figure 6. Current transients obtained at a 10-μm-diameter Pt tip by application of the 20 ms potential pulse of –0.5-V magnitude to the 1-mm-diameter Pt disk (substrate). Solution was 5 mM in $Ru(NH_3)_6^{3+}$ and 0.5 M in KNO_3. Initially, both the tip and the substrate potentials were 0 V vs SCE. Tip–substrate separation was 34.9 μm. Triangles represent the transient obtained without filtering; solid line obtained with filter frequency of 25 Hz. The initial current spikes are due to capacitive coupling between the tip and the substrate.

This regime, however, it not suitable for our experiments because the unavoidable small uncertainties in the tip position relative to the film/solution interface and film thickness would cause significant errors at small d. Moreover, the tip current at very short (submicrosecond) times after the application of the potential pulse to the substrate is disturbed by capacitive coupling between the electrodes.[30] A similar effect is observed in experiments with interdigitated arrays where the application of a potential pulse to the generator microelectrode leads to a current spike at closely spaced collector electrodes. Thus the calibration curves, t_{max} vs d^2, were obtained for tip–substrate separations larger than a. To determine the const corresponding to the SECM geometry (and also to check the validity of eq 12 for SECM conditions), we obtained t_{max} vs d^2 curves for a system with a known D, the reduction of $Ru(NH_3)_6^{3+}$, at a 1-mm-diameter Pt substrate with the collection of $Ru(NH_3)_6^{2+}$ at a 10-μm-diameter Pt tip electrode. This model experimental system was chosen because of its mechanistic simplicity and well-known value of the diffusion coefficient. Two experimental parameters need to be defined for these measurements, the pulse width and the time constant of the potentiostat current follower circuit. The pulse width, Δt, should be sufficiently small to ensure the independence of t_{max} on this parameter. Our measurements, in agreement with those in ref 14c, showed that t_{max} remained essentially constant for various Δt values within the interval $0.05t_{max} \leq \Delta t \leq 0.2t_{max}$ (see Table I). The use of shorter pulses was limited by the tip current, which was quite low in these experiments. This latter problem was diminished by using the low-pass filter on the potentiostat to allow more precise evaluation of t_{max} (Figure 6). One can see from Table I and Figure 6 that filtering did not influence the value of t_{max} within the range of experimental uncertainty. In general, we chose Δt as low, and the filter frequency as high, as possible without great distortions of transients by noise.

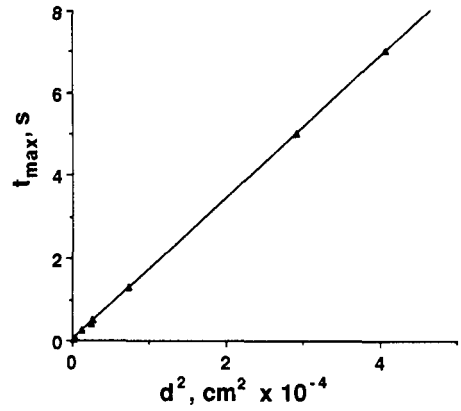

Figure 7. Time corresponding to the maximum tip current as a function of squared tip–substrate distance. Triangles were obtained by averaging experimental results with different pulse durations and filter frequencies. Experimental conditions as in Figure 6.

The value of const = 0.11 was found from the slope of the calibration line at different values of d (Figure 7). The difference between this value and that in ref 5c is attributed to the microdisk-shaped collector electrode. The calibration curve is linear over a range of d of 8–200 μm, corresponding to a d/a variation from 1.6 to 40. Thus, this const value should apply over the same d/a range for any size of the SECM tip.

Evaluation for the Br^- Diffusion Coefficient in a Solid AgBr Film. Transient measurements with the Ag/AgBr substrate were carried out by a similar procedure to that described above. The 10-μm-diameter Pt tip, initially biased at –0.5 V vs SCE, was positioned in close proximity to the substrate by noting the i_T obtained with $Ru(NH_3)_6^{3+}$ mediator. In these experiments, direct contact between the tip and the substrate was avoided to prevent AgBr reduction at the negatively biased tip electrode. After positioning, the tip potential was changed to +0.9 V vs SCE, a value sufficiently positive for diffusion-limited bromide ion oxidation. After the application of a negative potential pulse to the Ag/AgBr electrode, one could observe the current transient at the substrate (Figure 3B), indicating the reduction of silver bromide:[21]

$$AgBr + e = Ag + Br^- \qquad (13)$$

with the liberation of Br^- into solution. The high resistivity of AgBr suggests that the reduction should start at the boundary of the AgBr layer with the Ag substrate. The bromide anions diffuse to the outer boundary of the layer, move into solution and ultimately cross the interelectrode gap, and are oxidized at the tip electrode. Thus, the diffusion coefficient characterizing the speed of the Br^- movement in the AgBr lattice can be determined using the tip transient analysis described above.

Before the application of a potential pulse to the substrate, the tip was positioned at a distance of 3–4 μm from the AgBr/solution boundary. Since the Br^- diffusion coefficient in aqueous solution is about 2×10^{-5} cm^2/s,[31] the contribution of the solution diffusion to t_{max} will be of the order of 1 ms, i.e., much smaller than the experimentally measured value. The bromide diffusion coefficient found from the calibration curve (Figure 8) with const = 0.11 was $D = 5.6 \times 10^{-7}$ cm^2/s. This value is about 35 times lower than D in aqueous solution and is thus attributed to Br^- diffusion in AgBr. It is significantly higher than the diffusion coefficient of a foreign species (e.g., $Os(bpy)_3^{3+}$) in this compact solid film, suggesting that this represents specific bromide lattice diffusion in AgBr, rather than mass transfer within pores in the film. The independence of D for Br^- with film thickness for a given potential step magnitude (Figure 8) suggests that the contribution of any electrical field (migrational) effect to mass transfer is unimportant.

Clearly, similar measurements can be carried out with the electroactive species generated at the tip and collected at the

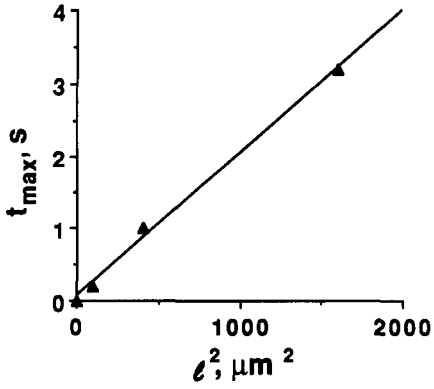

Figure 8. Calibration curve for the determination of the Br^- diffusion coefficient in AgBr. Tip current transients were obtained by applying a potential pulse of -0.5-V magnitude to a 1-mm-diameter Ag/AgBr disk (initially at 0 V vs SCE). Pulse durations were 50, 100, and 200 ms for layer thickness of 10, 20, and 40 μm, respectively.

substrate. This approach may be advantageous when substrate biasing is not desirable (e.g., with a conducting polymer whose morphology is potential dependent). Another useful modification would be measurements with the tip in direct contact with the film/solution interface. This might be necessary if the species of interest could not leave the film.

Conclusions

We have described several SECM-based procedures for characterization of thin electroactive films. From the shape of the tip current–distance curve one can find the locale of the source of the SECM feedback, i.e., the place where any heterogenous chemical or electrochemical reaction occurs. The evaluation of the rate constants for such chemical reactions can be obtained by straightforward extensions of SECM theory. As an example, we demonstrated that the oxidation of $Ru(NH_3)_6^{2+}$ proceeds via chemical rather than electrochemical reaction at the AgBr/solution interface with a rate constant of 0.082 cm/s.

The proposed determination of the diffusion coefficient of species inside a solid film is similar to procedures based on sandwich-type devices[14c] and interdigitated arrays.[27] However, unlike those techniques, the SECM measurements do not require incorporation of the film into a sandwich configuration, e.g., by casting it on top of a microelectrode array, and they allow the determination of diffusion coefficients for counterions leaving (or entering) the film and offer a more symmetrical geometry. The diffusion coefficient of bromide anions inside a AgBr layer was found to be 5.6×10^{-7} cm^2/s, i.e., about 35 times smaller than the analogous value in aqueous solution. The described procedures should also be useful for studies of electrodes modified with electronically and ionically conductive polymers as well as with nonelectroactive thin coatings and films (e.g., clays, zeolites).

Acknowledgment. The support of this research by grants from the National Science Foundation (CHE 9214480) and the Robert A. Welch Foundation is gratefully acknowledged. M.A. acknowledges financial support from the Islamic Development Bank Merit Scholarship Program. Our thanks to Drs. F.-R. F. Fan and B. R. Horrocks for helpful discussions.

References and Notes

(1) (a) Murray, R. W. In *Electroanalytical Chemistry*; Bard, A. J., Ed.; Marcel Dekker: New York, 1984; Vol. 13, p 191. (b) Hillman, A. R. In *Electrochemical Science and Technology of Polymers*; Lindford, R. G., Ed.; Elsevier, New York, 1987; p 103. (c) Inzelt, G. In *Electroanalytical Chemistry*; Bard, A. J., Ed.; Marcel Dekker: New York, 1994; Vol. 18, p 89.

(2) Bard, A. J.; Fan, F.-R. F.; Mirkin, M. V. In *Electroanalytical Chemistry*; Bard, A. J., Ed.; Marcel Dekker: New York, 1994; Vol. 18, p 243.

(3) Unwin, P. R.; Bard, A. J. *J. Phys. Chem.* **1992**, *96*, 5035.

(4) (a) Kwak, J.; Anson, F. C. *Anal. Chem.* **1992**, *64*, 250. (b) Lee, C.; Anson, F. C. *Anal. Chem.* **1992**, *64*, 528.

(5) (a) Pierce, D. T.; Unwin, P. R.; Bard, A. J. *Anal. Chem.* **1992**, *64*, 1795. (b) Horrocks, B. R.; Mirkin, M. V.; Pierce, D. T.; Bard, A. J.; Nagy, G.; Toth, K. *Anal. Chem.* **1993**, *65*, 1213.

(6) Xie, Y.; Anson, F. C. *J. Electroanal. Chem. Interfacial Electrochem.* **1993**, *349*, 325.

(7) Kwak, J.; Bard, A. J. *Anal. Chem.* **1989**, *61*, 1221.

(8) Sharp, M.; Lindhom, B.; Lind, E. L. *J. Electroanal. Chem. Interfacial Electrochem.* **1989**, *274*, 35.

(9) Bard, A. J.; Mirkin, M. V.; Unwin, P. R.; Wipf, D. O. *J. Phys. Chem.* **1992**, *96*, 1861.

(10) Mirkin, M. V.; Richards, T. C.; Bard, A. J. *J. Phys. Chem.* **1993**, *97*, 7672.

(11) Leddy, J.; Bard, A. J.; Maloy, J. T.; Savéant, J. M. *J. Electroanal. Chem. Interfacial Electrochem.* **1985**, *187*, 207 and references therein.

(12) Anson, F. C.; Blauch, D. N.; Savéant, J. M.; Shu, C.-F. *J. Am. Chem. Soc.* **1991**, *113*, 1922.

(13) Sharp, M.; Lindom, B.; Lind, E. L. *J. Electroanal. Chem. Interfacial Electrochem.* **1993**, *345*, 223.

(14) (a) Wooster, T. T.; Longmire, M. L.; Zhang, H.; Watanabe, M.; Murray, R. W. *Anal. Chem.* **1992**, *64*, 1132 and references therein. (b) Chidsey, C. E. D.; Feldman, B. J.; Lundgren, C.; Murray, R. W. *Anal. Chem.* **1986**, *58*, 601. (c) Feldman, B. J.; Feldberg, S. W.; Murray, R. W. *J. Phys. Chem.* **1987**, *91*, 6558.

(15) (a) Pickup, P. G.; Murray, R. W. *J. Am. Chem. Soc.* **1983**, *105*, 4510. (b) Burgmayer, P.; Murray, R. W. *J. Phys. Chem.* **1984**, *88*, 2515.

(16) Mirkin, M. V.; Fan, F.-R. F.; Bard, A. J. *Science* **1992**, *257*, 364.

(17) Gaudiello, J. G.; Sharp, P. R.; Bard, A. J. *J. Am. Chem. Soc.* **1982**, *104*, 6373.

(18) Bard, A. J.; Fan, F.-R. F.; Kwak, J.; Lev, O. *Anal. Chem.* **1989**, *61*, 1794.

(19) Wipf, D. O.; Bard, A. J. *J. Electrochem. Soc.* **1991**, *138*, 496.

(20) *CRC Handbook of Chemistry and Physics*; Lide, D. R., Ed.; CRC Press: Boca Raton, FL, 1990; p 4–100.

(21) Lal, H.; Thirsk, H. R.; Wynne-Jones, W. F. K. *Trans. Faraday Soc.* **1951**, *47*, 70.

(22) Mirkin, M. V.; Fan, F.-R. F.; Bard, A. J., manuscript in preparation.

(23) Mirkin, M. V.; Bard, A. J. *Anal. Chem.* **1992**, *64*, 2293.

(24) Hubbard, A. T.; Anson, F. C. In *Electroanalytical Chemistry*; Bard, A. J., Ed.; Marcel Dekker: New York, 1970; Vol. 4, p 129.

(25) Mirkin, M. V.; Fan, F.-R. F.; Bard, A. J. *J. Electroanal. Chem. Interfacial Electrochem.* **1992**, *328*, 47.

(26) Wightman, R. M.; Wipf, D. O. In *Electroanalytical Chemistry*; Bard, A. J., Ed.; Marcel Dekker: New York, 1989; Vol. 15, p 267.

(27) (a) Licht, S.; Cammarata, V.; Wrighton, M. S. *J. Phys. Chem.* **1990**, *94*, 6133. (b) Tatistcheff, H. B.; Fritsch-Faules, I.; Wrighton, M. S. *J. Phys. Chem.* **1993**, *97*, 2732.

(28) Bard, A. J.; Denuault, G.; Friesner, R. A.; Dornblaser, B. C.; Tuckerman, L. S. *Anal. Chem.* **1991**, *63*, 1282.

(29) Bard, A. J.; Faulkner, L. R. *Electrochemical Methods*; John Wiley & Sons: New York, 1980; p 129.

(30) Bard, A. J.; Fan, F.-R. F.; Kwak, J.; Lev, O. *Anal. Chem.* **1989**, *61*, 132.

(31) Parson, R. *Handbook of Electrochemical Constants*; Butterworth: London, 1959; p 79.